Resource

Cell Reports

# Single-Cell Transcriptomics Analyses of Neural Stem Cell Heterogeneity and Contextual Plasticity in a Zebrafish Brain Model of Amyloid Toxicity

## Graphical Abstract

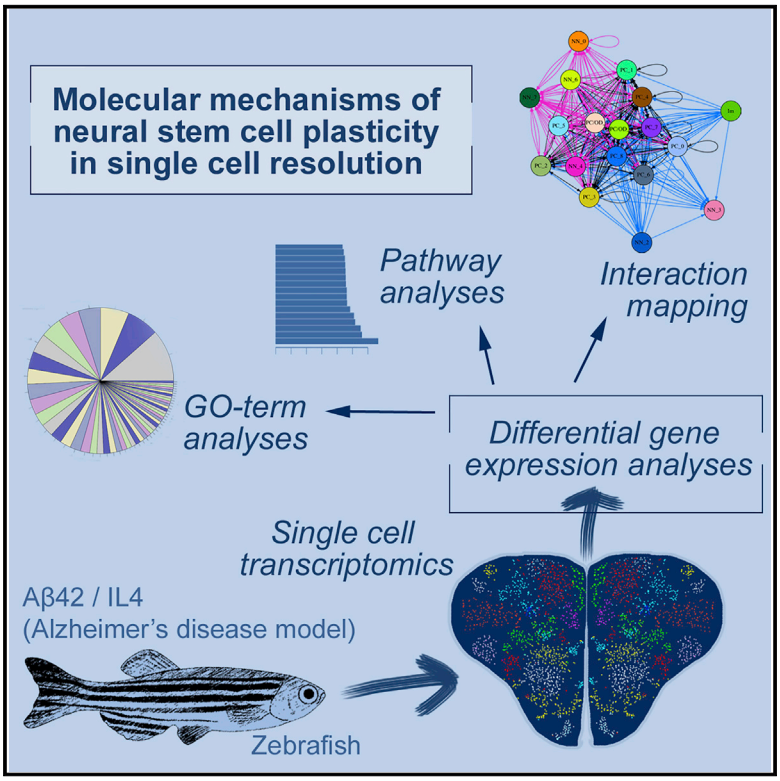


## Authors

Mehmet Ilyas Cosacak, Prabesh Bhattarai, Susanne Reinhardt, Andreas Petzold, Andreas Dahl, Yixin Zhang, Caghan Kizil

## Correspondence

mehmet.cosacak@dzne.de (M.I.C.), caghan.kizil@dzne.de (C.K.)

## In Brief

The zebrafish brain combats Alzheimer's disease by producing more neurons, which are derived from neural stem cells. By using single-cell sequencing technology, Cosacak et al. identify distinct stem cell populations that react differently to Alzheimer's disease-like conditions in the adult zebrafish brain and develop tools to investigate their molecular programs.

## Highlights

- Single-cell transcriptomics reveals neural stem cell/glia heterogeneity in zebrafish
- Different stem cell populations can be defined spatially and molecularly
- Amyloid-β-42 and interleukin-4 induce plasticity of certain progenitor populations
- Interaction mapping predicts the pathways that regulate neural stem cell plasticity

Cosacak et al., 2019, Cell Reports *27*, 1307–1318
April 23, 2019 
https://doi.org/10.1016/j.celrep.2019.03.090

CellPress

Cell Reports
Resource



# Single-Cell Transcriptomics Analyses of Neural Stem Cell Heterogeneity and Contextual Plasticity in a Zebrafish Brain Model of Amyloid Toxicity

Mehmet Ilyas Cosacak,[1,*] Prabesh Bhattarai,[1] Susanne Reinhardt,[2] Andreas Petzold,[2] Andreas Dahl,[2] Yixin Zhang,[3] and Caghan Kizil[1,4,5,6,*]
[1]Kizil Lab, German Center for Neurodegenerative Diseases (DZNE) Dresden, Helmholtz Association, Tatzberg 41, 01307 Dresden, Germany
[2]DRESDEN-concept Genome Center, Center for Molecular and Cellular Bioengineering (CMCB), Technische Universität Dresden, Fetscherstr. 105, 01307 Dresden, Germany
[3]B CUBE, Center for Molecular Bioengineering, TU Dresden, Tatzberg 41, 10307 Dresden, Germany
[4]Kizil Lab, Technische Universität Dresden, Center for Regenerative Therapies Dresden (CRTD), Fetscherstr. 105, 01307 Dresden, Germany
[5]Twitter: @CaKizil
[6]Lead Contact
*Correspondence: mehmet.cosacak@dzne.de (M.I.C.), caghan.kizil@dzne.de (C.K.)
https://doi.org/10.1016/j.celrep.2019.03.090

## SUMMARY

**The neural stem cell (NSC) reservoir can be harnessed for stem cell-based regenerative therapies. Zebrafish remarkably regenerate their brain by inducing NSC plasticity in a Amyloid-β-42 (Aβ42)-induced experimental Alzheimer's disease (AD) model. Interleukin-4 (IL-4) is also critical for AD-induced NSC proliferation. However, the mechanisms of this response have remained unknown. Using single-cell transcriptomics in the adult zebrafish brain, we identify distinct subtypes of NSCs and neurons and differentially regulated pathways and their gene ontologies and investigate how cell-cell communication is altered through ligand-receptor pairs in AD conditions. Our results propose the existence of heterogeneous and spatially organized stem cell populations that react distinctly to amyloid toxicity. This resource article provides an extensive database for the molecular basis of NSC plasticity in the AD model of the adult zebrafish brain. Further analyses of stem cell heterogeneity and neuro-regenerative ability at single-cell resolution could yield drug targets for mobilizing NSCs for endogenous neuro-regeneration in humans.**

## INTRODUCTION

Zebrafish, with their extensive regenerative ability, have become a key model organism for studies of how tissues heal and regenerate (Alunni and Bally-Cuif, 2016; Kizil et al., 2012b; Zupanc, 2008). Although zebrafish provide valuable opportunities to molecularly dissect the regenerative programs in many tissues, there are still hurdles that render the interpretation of complex cellular interactions and responses difficult, such as the heterogeneity of progenitor cell populations and their differential response to stimuli (März et al., 2010).

Neural progenitor cells can have various identities in vertebrates (Alvarez-Buylla et al., 2002). During development of the nervous system, the neuroectoderm gives rise to neurons through the earliest neural progenitors that have the neuroepithelial character (Klämbt, 2012; Pacary et al., 2012). Later, the neuroepithelium gives rise to radial glial cells, which remain the primary progenitor cell type in lower vertebrates such as zebrafish but are replaced by astrocytes in mammals (Goldman, 2012; Götz, 2012; Kriegstein and Alvarez-Buylla, 2009; Pollen et al., 2015). These two glial cell types are also neurogenic. For instance, in the subventricular zone of the mouse brain, the primary neurogenic progenitors are astrocytes (Doetsch, 2003; Doetsch et al., 1999), whereas, in the zebrafish telencephalon, the analogous region, the pallium, is populated by radial glial cells, which are the neurogenic population (Adolf et al., 2006; Grandel et al., 2006; Kizil et al., 2012b; Than-Trong and Bally-Cuif, 2015; Zupanc, 2008). Therefore, investigation of the heterogeneity of stem cells in the adult zebrafish brain would provide an important understanding of how progenitor subtypes react to diseases, which molecular programs enable the plasticity of stem cells, and whether those programs could be harnessed for regenerative therapies in humans.

CNS regeneration in zebrafish is of particular importance because of the robust neural regeneration ability in zebrafish and potential clinical ramifications, which cannot be elucidated with mammalian models. The zebrafish brain has a widespread constitutive proliferative ability, and radial glial cells (RGCs) constitute the major stem cell population. In the telencephalon, for instance, RGCs form neurons throughout the life of the zebrafish, and they also respond to neuronal loss by reactively proliferating. This proliferation requires induced molecular programs that are required for the special regenerative ability of these stem cells. Different insults have been shown to affect the stem cell response differently, suggesting that distinct progenitor cell populations might differentially react upon stimuli. For instance, we generated an amyloid toxicity model in the adult zebrafish brain and identified that zebrafish can effectively enhance neural progenitor cell proliferation and neurogenesis by inducing interleukin-4 (IL-4), which mediates the crosstalk

between disease pathology in neurons to initiate the regenerative output in stem cells (Bhattarai et al., 2016, 2017a, 2017b; Kizil, 2018). We also found that IL-4 can directly affect human neural stem cells in a similar fashion to induce proliferative and neurogenic ability (Papadimitriou et al., 2018). However, in traumatic injuries, IL-4 is not induced in the zebrafish brain, although stem cell proliferation increases in both situations. Therefore, there is a need to define the relationship of stem cell heterogeneity and the regenerative plasticity response of those stem cells in the zebrafish brain. This would provide a context-dependent understanding of the molecular programs underlying the regenerative ability rather than a one-size-fits-all approach.

Because of the heterogeneity of stem cell populations and neuronal subtypes in the zebrafish brain, it has not been possible to clearly delineate cell-type-specific responses. This was also the case for the Alzheimer's disease model, where it remained unknown how Amyloid-β-42 (Aβ42) and IL-4 lead to enhanced stem cell plasticity and neurogenesis, which individual subtypes of stem cells and neurons respond to Aβ42 and IL-4, and how individual the responses were. Therefore, in our study, we performed single-cell sequencing in control, Aβ42-treated, and IL-4-treated adult zebrafish telencephalon and categorized the cell type identities and molecular programs of individual cell types, how Aβ42 and IL4 altered those programs, and how different cell types interacted with each other. Our results add further elaboration to our previous findings that Aβ42 and IL-4 affect neural stem cells to enhance their neurogenic capacity by providing detailed analyses of heterogeneous cell populations. We believe that the extensive datasets will not only provide a useful resource for detailed examination of the adult zebrafish brain and its remarkable regenerative ability in a homeostatic and neurodegenerative context but also serve as an improvable database for further research regarding the regenerative ability of vertebrate brains.

## RESULTS AND DISCUSSION

### Sequencing and Clustering of Cells to Identify Main Cell Types

Previously, we have shown that Aβ42 toxicity in zebrafish induces the expression of IL-4 and that the IL-4-STAT6 pathway induces neural stem- progenitor cell (NSPC) proliferation (Bhattarai et al., 2016, 2017a, 2017b). We also found that IL-4 can directly affect human neural stem cells in a similar fashion to induce proliferative and neurogenic ability (Papadimitriou et al., 2018). To investigate which cell types respond to Aβ42 and IL-4 in the adult zebrafish brain, we injected PBS, Aβ42, and IL-4 into a 6-month-old adult zebrafish brain as described previously (Bhattarai et al., 2016) and designed an analysis pipeline (Figure 1A). We dissected the telencephalon region of the adult brain of a transgenic zebrafish that expressed GFP under the *her4.1* promoter, which marks glial cells (Yeo et al., 2007). Using flow cytometry-assisted cell sorting, we removed cell debris and dead cells (Figures S1A–S1C) and enriched the GFP+ and GFP− cells. To perform single-cell sequencing, we mixed viable GFP+ and GFP− cells in a 1:1 ratio. After single-cell sequencing, we mapped the resulting reads to the zebrafish genome and performed unbiased clustering (Figures 1B–1D) using Seurat software (Butler et al., 2018). After removing cells with minimum and maximum thresholds for nUMI, nGene, and mitochondrial RNA genes, we obtained 609, 737, and 450 cells from PBS-, Aβ42-, and IL-4-treated fish telencephalons, respectively. The read numbers per cell (nUMI), number of genes detected per cell, and mitochondrial mRNA percentages (Figures S1D–S1I) were comparable with previously published datasets (Farrell et al., 2018; Pandey et al., 2018; Raj et al., 2018; Satija et al., 2015), supporting the quality of our datasets. Furthermore, by comparing nUMI, nGene, percent.gfp (percentage of gfp transcripts), and percent.mito (percentage of mitochondrial genes), our datasets were comparable with each other (Figures S1D–S1I). By using the Seurat feature of integrating data analyses from different conditions, we classified our cell types for all samples together (Figures 1B and 1C; Figures S1J and S1K). By integrating and combining all cells, we were able to classify cell types that have fewer cells in one sample; otherwise, these cell types are classified with the closest cell types based on the variable genes (data not shown). By using some marker genes (e.g., *lcp1*, *pfn1*, *her4.1*, *s100b*, *id1*, *sv2a*, *nrgna*, *olig1*, and *olig2*; Figure S1L), we identified 4 major cell clusters as Im (immune) cells, PCs (progenitor cells), NNs (neurons), and OPCs/ODs (oligodendrocyte progenitor cells and oligodendrocytes). Then, we identified the top 10 markers for each of these 4 clusters (OPCs/ODs not combined, kept as OPC/OD_1 and OPC/OD_2) (Figure 1D) and top 10 marker genes (Figure 1E; Data S1).

Given that Aβ42 and IL-4 have effects on gene expression, we asked whether combining all cells from different conditions would affect cell clustering. Because Seurat can be used to cluster cells from different treatments, technologies, or species (Butler et al., 2018), we observed a clear separation of marker genes in two main cell clusters: NNs and PCs. Interestingly, the top 10 marker genes in NNs are almost completely absent in PCs and vice versa (Figure 1E). Moreover, the majority of neuronal markers are absent in immune cells, suggesting that cluster-based cell separation is successful.

The PCs express some commonly known marker genes such as *fabp7a*, *her4.1*, *her4.2*, and *id1* (Figure 1E). Interestingly, *fabp7a* is found in all PCs, and *her4.1* is not expressed by all PCs, possibly sparing non-glial progenitors such as the neuroepithelium (Figure S1L). Of note, as expected, GFP is expressed in almost all *her4*.1 cells at higher levels (Figure 2C; Figure S2K).

### Cell Clustering and Identification of Cell Types for PCs and NNs

After several rounds of analyses, we realized that variable genes in NNs and PCs limit the clear separation of cells. Thus, while finding the top marker genes for PCs by comparing genes from one cell cluster with all other cell clusters (Ims, OPCs, and NNs), we found that marker genes cannot be clearly separated or that one marker genes are shared with 2 or more other PCs. To find subtypes of PCs, we ran clustering using only PCs identified in Figure 1 and using the same analysis steps described above, except for using the ''num.dims'' value (an indicator of the number of dimensions used for the principal-component analyses) as 20 to increase the stringency for aligning and finding the iterative clusters (Figure 2A; Figures S2A-S2C and S2H). With the same strategy, we further sub-clustered the NNs as

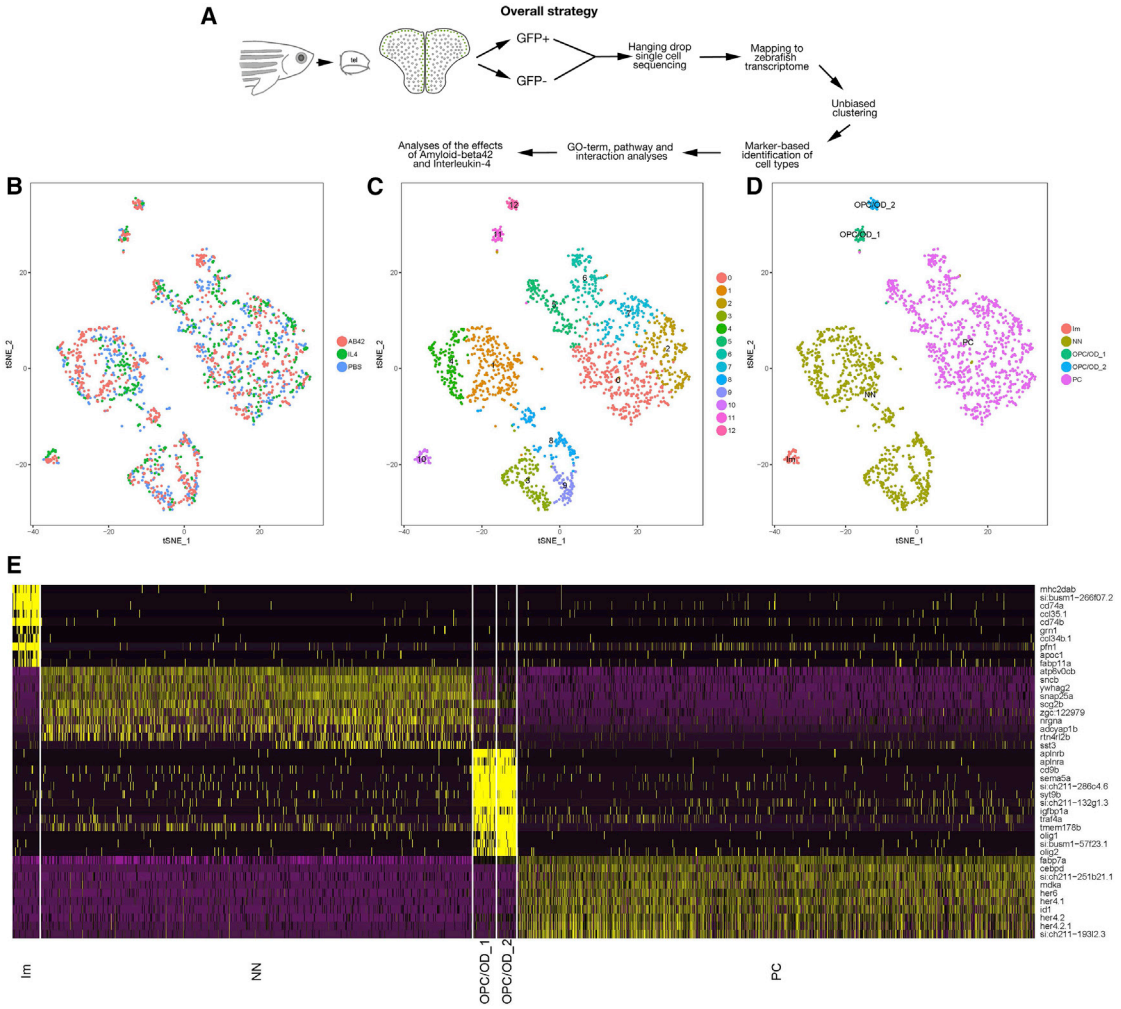


**Figure 1. Cell Sorting and Categorization of Cell Types**

(A) Overall strategy for cell sorting and single-cell data analyses.

(B–D) tSNE clustering of cells.

(B) Co-existence map of cells from PBS, Aβ42, and IL-4-treated brains on tSNE plots.

(C) Cell clusters identified by resolution 1.

(D) The main cell clusters are color-coded for immune (Im) cells, progenitor cells (PCs), neurons (NNs), and oligodendrocytes/progenitor cells (OPC/OD_1 and OPC/OD_2).

(E) Heatmap of the top 10 markers for the main cell clusters.

One dissected brain was used for every experiment. See also Figures S1 and S2.

well (Figures S2D-S2F and S2I). We then color-coded cell clusters for PCs and NNs (Figures S2C and S2F) and showed the cells on a t-distributed stochastic neighbor embedding (tSNE) plot (Figure 1A) using the new color-coded cells (Figure S2G). With this strategy, we observed better marker enrichment in the PC and NN types through iterative sub-clustering (Figures S2J and S2K; https://www.kizillab.org/singlecell).

Interestingly, after sub-clustering the PCs and neuronal cells, some cell clusters that are mixed by using all cells are clearly separated by iterative sub-clustering. For instance, cell clusters 1 and 4 in Figure 1C can be clustered into 4 neuronal clusters (NN_0, NN_1, NN_4, and NN_7; Figures S2F and S2G). Additionally, by using all cells, we could identify PC 0, PC 1, PC 2, and PC 4 cells and clearly separate them in tSNE plots (Figure 2A; Figure S2C). Therefore, we propose that iterative sub-clustering of PCs is an efficient way to demonstrate the heterogeneity of similar cell types.

In the current study, we focused mainly on PCs and the effect of Aβ42 and IL-4 on those cells; however, wherever required, we provide results from all cell types as well (https://www.kizillab.org/singlecell). After the two-step clustering, we identified 1, 2, 8, and 9 cell clusters for Im cells, OPCs/ODs, NNs, and PCs, respectively (Figure S2G) and focused mainly on PCs. After identifying PC clusters, we aimed to validate our results with biological *in situ* data to predict the regionalization and type of PCs. Therefore, we took the advantage of an unbiased and

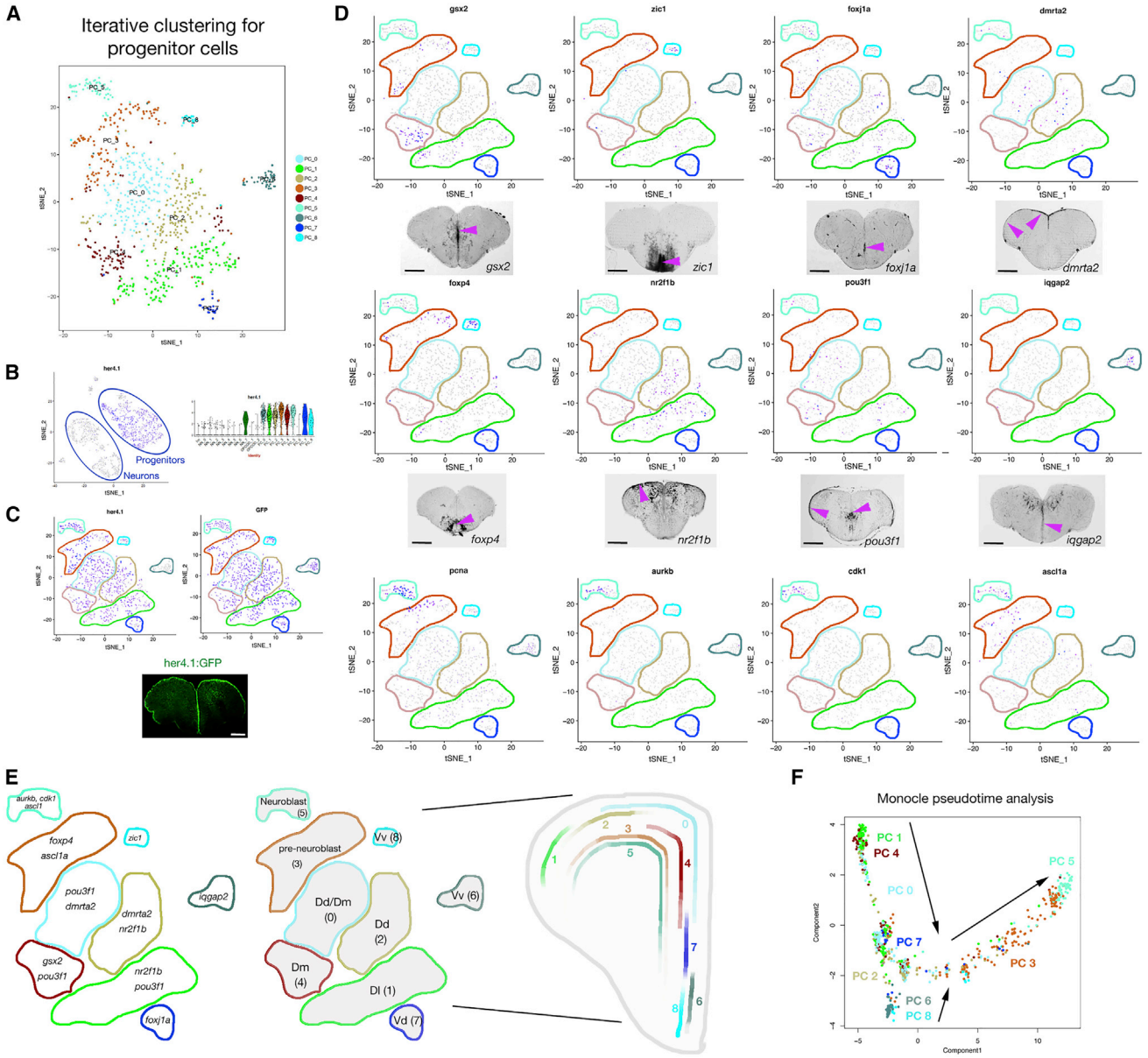


**Figure 2. Identification of PC Types**

(A) tSNE plots for PC clusters.

(B) *her4.1* expression in a tSNE (left) and violin plot (VLN) of single cell data (right), which contain all cell types.

(C) her4.1 expression (left) and GFP expression (right), shown in tSNE plots for PCs. Also shown is her4.1-driven GFP staining on a telencephalon section (bottom).

(D) tSNE plots for some of the marker genes and relevant *in situ* hybridizations. Pink arrowheads denote expression domains.

(E) Marker genes and localization of cell types on a representative telencephalic scheme.

(F) Cell trajectories on pseudotime generated by monocle2; all colors depict the cell cluster colors in (A).

Scale bars, 200 μm. See also Figures S1–S3.

independent study that is comprehensively documented as a public repository, The Atlas of Gene Expression in the Telencephalon of Adult Zebrafish (AGETAZ) (https://itgmv3.itg.kit.edu/agetaz/index.php; Diotel et al., 2015).

We tested the validity and reliability of our tSNE feature plots by comparing her4.1 and GFP plots with GFP expression in the her4.1-GFP transgenic zebrafish line (Figure 2B) and observed that, indeed, GFP is a general indicator of PC populations (Figure 2C). Later, we selected several regional markers from the *in situ* hybridization database and checked their localizations on feature plots (Figure 2D; Figure S3). As a result, we identified deterministic marker expression for all PC clusters (Figure 2D).

For instance, PC 5 cells express *pcna*, *mki67*, *top2a*, and *ascl1a*, indicating that these cells are actively proliferating cells or neuroblasts. PC 3 cells are the closest cells to PC 5 cells by expressing *pcna* and *ascl1a* but not *mki67* and *top2a* and can be classified as non-proliferating neuroblast precursors or pre-neuroblasts (Figure 2D; Figures S2J). Pre-neuroblasts and neuroblasts share common top marker genes (Figure S2J). Neuroblasts express known markers associated with the neuroblast state (such as *pcna*, *stmn1a*, and *hmgb2*) at higher levels compared with pre-neuroblasts. These two cell types do not show a regional localization but are scattered along the ventricular region in the adult zebrafish telencephalon (Figure 2D).

PC 6 cells do not express *s100b* and *her4.1*, whereas PC 8 cells express *her4.1* but not *s100b*. These two cells are not radial glial cells but, combined with the expression of other markers (e.g., *zic1*, *krt8*, and *clu*; Figure 2D; Figure S3) can be classified as neuroepithelium cells. These cells are mainly localized in the ventral (Vv) telencephalon (based on *zic1* and *iqgap2* expression; Figure 2D). Even though these clusters localize similarly to the ventral telencephalon, they represent two distinct populations.

PC 0 contains cells that express markers of the dorsal (Dd) and dorsomedial (Dm) part of the telencephalon (Figure 2; *pou3f1* and *dmrta2*). Although PC 2 cells express *dmrta2* and *nr2f1b* (Dd markers; Figure 2D), PC 4 cells express *gsx2* and *pou3f1*, which are expressed more in the Dm region (Figure 2D). Interestingly, PC 0 shares common markers either with PC 2 or PC 4. Based on the presence and expression of these marker genes, we classify PC 2 as Dd, PC 4 as Dm and PC 0 as both Dd and Dm. These findings indicate that different regions contain heterogeneous PC populations that differ by marker gene expression.

PC 1 expresses *nr2f1b* and *pou3f1* and, based on the *in situ* hybridization results of these genes, mainly localize on the lateral part of the telencephalon (dorsolateral [Dl]). PC 7 marks an interesting cell type that is characterized by *foxj1a* expression, which is clearly localized to the interstitial region between the ventral and Dm telencephalon (Figures 2D and 2E), and is classified as cells at the ventral part of the dorsal telencephalon (Vd). *foxj1a* is a central regulator of motile ciliogenesis and is co-expressed in PC 7 with *rsph9*, *cfap126*, and *enkur*, which are motile ciliated cell markers (Figure S3) (Lindsey et al., 2012; Ogino et al., 2016). Based on our findings, we propose that PC 7 corresponds to ependymal cells of the adult zebrafish telencephalon. Because ciliated cells are crucial for the development and function of the CNS (Olstad et al., 2019; Sternberg et al., 2018), and because the neurogenic nature of ependymal cells is controversial (Johansson et al., 1999; Spassky et al., 2005), our results provide important molecular information in a normal and Alzheimer's-like state and could contribute to more sophisticated elaboration of the neurogenic capacity and physiological functions of ependymal cells.

Overall, marker genes, *in situ* expression, and differential clustering reveal that the ventricular region of adult zebrafish telencephalon contains distinct progenitor subtypes that can be spatially defined (Figure 2E).

By using iterative sub-clustering of PCs, we identified 7 progenitor and 2 neuroblast types in the telencephalon. To identify how these cell types are related to each other, we constructed a pseudotime using Monocle software (Qiu et al., 2017; Figure 2F). We found that PCs perfectly progressed from progenitor states toward proliferative states (Figure 2F). PC 0, 1, 2, and 4 are distributed on pseudotime but not in a specific location. This indicates that progenitors have a physiological continuum from non-dividing (or quiescent) to potentially dividing states. Pseudotime also predicts the formation of pre-neuroblasts and neuroblasts from other PCs, and, interestingly, regardless from which progenitor state they come, neuroblasts are rather homogeneous cell types in terms of marker gene expression. Based on this observation, we propose that, by using pseudotime, we could also capture the state of PCs and that neurogenic heterogeneity exists at the PC stage rather than at the neuroblast stage. We propose that the adult zebrafish brain contains committed and regionally specified neural progenitors that generate neurogenic diversity through a rather homogeneous neuroblast stage (all gene expression data, gene ontology (GO) term analyses, and tSNE plots for every cell cluster in control, amyloid-treated, and IL-4-treated brains can be found at https://www.kizillab.org/singlecell).

## Plasticity Is Affected in a Subset of PCs after Aβ42 and IL-4

Based on the spatially confined PC populations that display distinct marker gene expression, we hypothesized that some of these PC populations would react differentially to amyloid toxicity or IL-4 treatment. A central feature of neural progenitors is their plasticity, which would reflect in a proliferative response. To determine the cell types amyloid and IL-4 affect, we injected amyloid or IL-4 into adult zebrafish brains and analyzed cell proliferation in predefined regions: Dl, Dd, Dm, Vd, and Vv telencephalon (Figure 3A) by performing immunohistochemical staining for proliferating cell nuclear antigen (PCNA) and GFP on the her4.1:GFP transgenic reporter line (Figures 3B–3D'). We observed that amyloid and IL-4 increased cell proliferation in 3 of the 5 regions: the Dd, Dm, and Vd telencephalon (Figure 3E). These results suggest that PC populations react differentially to amyloid toxicity and that heterogeneity of the progenitors underlies neurogenic ability. Because the zebrafish brain can increase neurogenic output after various insults through activation of different molecular mechanisms (Alunni and Bally-Cuif, 2016; Bhattarai et al., 2016; Cosacak et al., 2015; Diotel et al., 2013; Kizil, 2018; Kizil et al., 2012a, 2012b, 2012c; Kyritsis et al., 2012; März et al., 2011; Shimizu et al., 2018; Tincer et al., 2016), understanding the subpopulation of PCs that are responsible for the regenerative ability after particular injuries would have tremendous clinical ramifications. More focused investigations of these special cells could shed light on which programs must be induced in comparative cell types in human brains to boost neurogenic output.

## Amyloid Toxicity Changes the Molecular Regulatory Landscape of PCs

Because amyloid toxicity affects PC plasticity in a spatially specific manner, we aimed to determine the molecular changes pertaining to this response using our single-cell analyses. Therefore, we determined differentially expressed genes (DEGs) in every cluster (Data S2) and subsequently identified differentially regulated Kyoto encyclopedia of genes and genomes (KEGG)

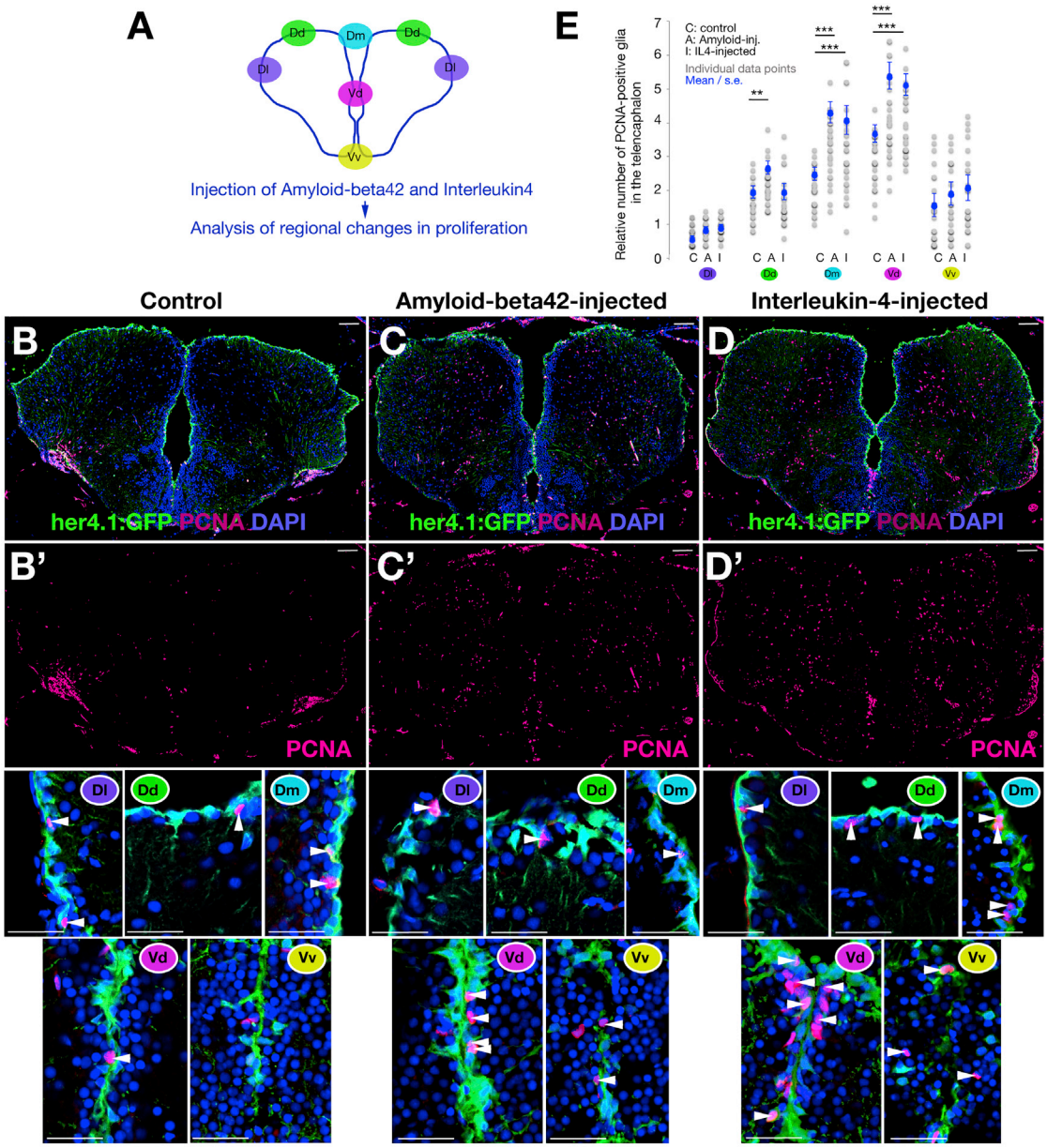


**Figure 3. Aβ42 and IL-4 Affect Specific Progenitor Populations in the Adult Zebrafish Brain**

(A) Schematic view of regionalization in the adult zebrafish telencephalon.

(B–D') Immunohistochemistry (IHC) staining for her4.1-driven GFP and PCNA on control (B), amyloid-injected (C), and IL-4-injected (D) telencephalic sections. In (B'), (C'), and (D'), PCNA channels are shown. Close-up views of GFP and PCNA double IHC are shown below the single channels. Regions are marked with color-codes as in (A). Scale bars, 50 μm.

(E) Quantification graph for the relative number of proliferating progenitors. Three brains were used for every experimental group. Data are represented as mean ± SEM. The levels of significance are *$p < 0.05$, **$p < 0.01$, and ***$p < 0.001$.

pathways in PCs that are located at the Dd, Dm, and Vd telencephalon (PC 0, 2, 3, 4, and 5; Figures 4A and 4B; Data S3). By comparing the DEGs in every cell cluster within individual treatments (i.e., Aβ42 and IL-4), we found that every cell type has a unique set of DEGs because the percent overlap of DEGs after Aβ42 or IL-4 treatment in a particular cell type is below 30% (percentage of the number of common DEGs in clusters X and Y divided by the number of DEGs in cluster X; Data S4A and S4B). However, when we compared the percent overlap of DEGs that are determined in a given cell type after Aβ42 and IL-4 treatment, we found that, in several cell types, Aβ42 and IL-4 lead to differential expression of more than 30% of the genes in a similar fashion (e.g., PC 0 cells, PC 4 cells, and Im cells; Data S4C). These results suggest that every cell type

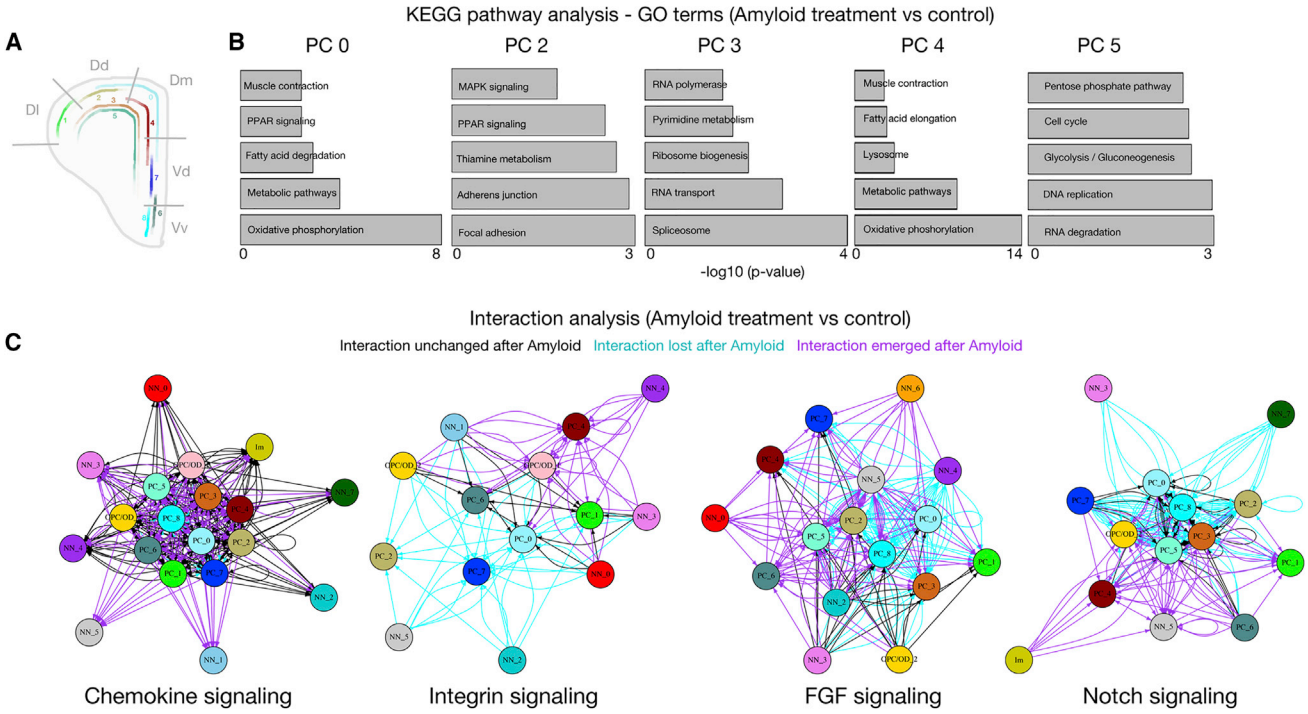


**Figure 4. Pathway Analyses and Interaction Maps for PC Populations Affected by Aβ42**

(A) Schematic view of the regional distribution of PCs in the adult zebrafish telencephalon.

(B) KEGG pathway analysis, indicating the 5 most affected pathways in PCs 0, 2, 3, 4, and 5.

(C) Representative interaction maps for chemokine, integrin, FGF, and Notch signaling. Black arrows, interactions present before and after amyloid treatment; cyan arrows, interactions lost after amyloid treatment; purple arrows, interactions emerging only after amyloid treatment.

See the Data S1, Data S2, Data S3, Data S4, and Data S5 for extensive datasets of GO terms, DEGs, and other interaction maps.

has a unique molecular signature that is synergistically affected by Aβ42 and IL-4.

With GO term analyses, we also observed that every cell cluster changed distinct molecular pathways after amyloid toxicity, with a few categories overlapping between cell clusters (e.g., oxidative phosphorylation). For instance, cell cycle-related pathways are affected by amyloid only in PC 5 (neuroblasts with proliferative ability), which supports our classification and suggests that, by investigating the differentially regulated pathways, we could determine the signaling landscape that is responsible for induced plasticity in particular cell types after amyloid toxicity. An example could be seen in PC 2, where the mitogen-activated protein kinase (MAPK) signaling pathway is uniquely affected (Figure 4B). Therefore, our single-cell data could be used to determine the signaling pathways that are specifically involved in regulation of neurogenic plasticity of particular PCs.

A prominent way in which cells interact with each other is through secreted molecules and their receptors in target cells. To determine such putative cell-cell communication through secreted molecules, we determined (bioinformatically and based on the literature) 646 ligands interacting with 658 receptors (Data S5). Among the marker genes expressed in clusters (Data S5), we found that 101 ligands and 117 receptors were expressed in identified clusters (Data S5). We generated several interaction maps based on identified genes (https://www.kizillab.org/singlecell; Data S5), portraying complex interaction between cell types.

Because the interaction data we obtained represent a potential interaction landscape based only on ligand-receptor pair interaction, it needed validation. Therefore, we determined the interaction of individual signaling pathways (https://www.kizillab.org/singlecell). Many major signaling pathways, such as fibroblast growth factor (Fgf), Integrin, chemokine, and Notch signaling, are known to be involved in cell-cell communication in the adult zebrafish brain (Alunni et al., 2013; Cacialli et al., 2016; Diotel et al., 2010; Jiao et al., 2011; Kaslin et al., 2009; Kizil et al., 2012a, 2012c; Shimizu et al., 2018). To depict how cell clusters interact using these pathways, we plotted the intercommunication predictions for cell types expressing the receptor or ligand for pathways (Figure 4C). We found that all interaction categories are complex and involve the participation of many cell types, which includes NN-PC and Im-PC interaction. Despite this complexity, such data mining could provide valuable and unprecedented biological information. We also identified other potential interactions with less studied ligands and receptors, such as *agrn*, *appa*, *ctgfa*, *gnai2*, *penkb*, *ptn*, *serpine*, *edil3a*, and *hbegf* (https://www.kizillab.org/singlecell), which might provide still unknown candidates for regulation of NSPC plasticity.

To provide biological verification of our interaction analyses, we selected the fibroblast growth factor (FGF) signaling pathway, which is involved in NCS/PC proliferation in the zebrafish brain

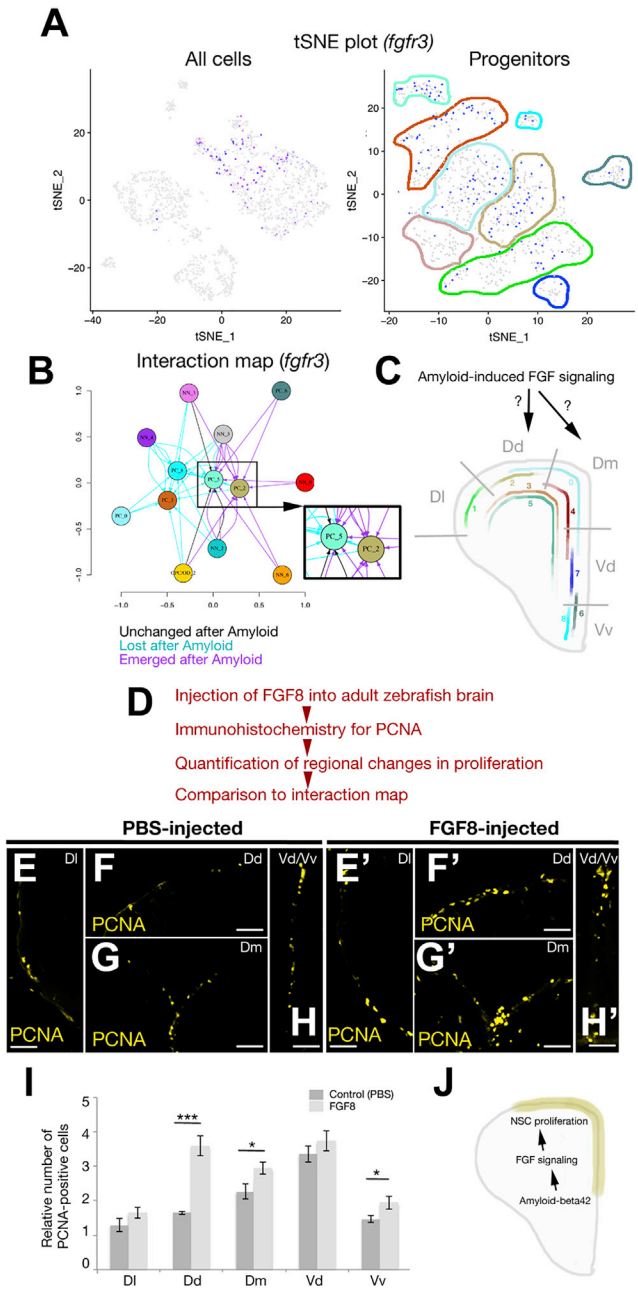


**Figure 5. Functional Investigation of Interaction Maps Reveals Fgf Signaling Controlling PC Proliferation**

(A) tSNE plot (all cells on the left, progenitors on the right) for *fgfr3*, which is localized specifically to PCs.

(B) Predicted interaction map for *fgfr3* and its ligands.

(C) Based on the interaction prediction, PC 2 and PC 5 are exposed to FGF signaling after amyloid treatment.

(D) Methodology for functional validation of the effects of FGF signaling on PC proliferation.

(E–H') Immunohistochemical staining for PCNA in control (E–H) and FGF8-injected (E'–H') adult zebrafish brains. Regional identities are indicated with the names denoted in (C). Panels E–H modified from Kizil and Brand, 2011.

(I) Quantification of regional proliferation response after FGF8-injection.

(J) Working model of the regulatory cascade of NSPC proliferation in the adult zebrafish brain by Aβ42-induced FGF signaling.

(Ganz et al., 2010; Kaslin et al., 2009; Kizil and Brand, 2011; Sleptsova-Friedrich et al., 2001; Topp et al., 2008), and investigated whether it would affect the proliferative ability of the brain regions that correspond to the cell clusters found to be affected by FGF in our interaction analyses (Figure 4C).

We performed tSNE plot analyses for all receptors for FGF (data not shown) and found that *fgfr3* is specifically expressed in PCs (Figure 5A). We then constructed an interaction map by determining the potential interactions through Fgfr3 (Figure 5B). With such a sub-interaction map, all possible communications through *fgfr3* and its ligands are sketched, and we hypothesized that Fgfr3 signaling would positively affect mainly PC 2 (Dd) and PC 5 (neuroblasts) (Figure 5C). Amyloid treatment seemed to cause interactions that were not present in control brains from various cell types toward PC 2 and PC 5 (Figures 5B and 5C). If the interaction map analyses were reliably predictive, then this would suggest that, after activation of Fgfr3 signaling upon Aβ42, the Dd and Dm regions of the zebrafish brain could change their proliferative response. To test this hypothesis, we injected the Fgfr3 ligand FGF8 (Chellaiah et al., 1999; Sleptsova-Friedrich et al., 2001) into the adult zebrafish brain and determined the changes in cell proliferation (Figure 5D) by performing immunohistochemical staining for PCNA (Figures 5E–5F'). We found that, compared with control brains, FGF8 injection significantly increased cell proliferation in the Dd and Dm regions, exactly as predicted by the interaction mapping (Figures 5G and 5H). Overall, our interaction studies provide an extensive high-resolution cell-cell communication map, and these predictions provides a further level of elucidation for the heterogeneity of neural stem cell populations and the molecular mechanisms controlling the plasticity response thereof.

Further investigation of our data and experimental validation of the candidates presented in our resource platform would provide the molecular programs underlying the neural stem cell (NSC) plasticity and regenerative response of the adult zebrafish brain in Alzheimer's disease conditions as well as the downstream regulation of IL-4. Given that we have recently shown that IL-4 is sufficient to enhance the human NSC plasticity and regenerative capacity in a 3D human Alzheimer's model and to circumvent the AD pathology (Papadimitriou et al., 2018), our data will undoubtedly provide more candidates that can be clinically relevant. Such an understanding would provide new therapeutic targets for Alzheimer's disease for clinical and pharmaceutical use, not only for neurogenesis but also for neuronal survival and synaptic integrity, as exemplified recently (Reinhardt et al., 2019).

## Conclusion

Heterogeneity of NSC activity and fate decisions mainly rely on activation or suppression of distinct molecular programs in respective cell types. Single-cell sequencing uniquely allows investigation of individual cell types and their response to stimuli. In our analyses, we identified distinct cell types of the adult zebrafish telencephalon, which is a widely used experimental

Three sections were quantified for every experimental group. Scale bars, 50 μm. Data are represented as mean ± SEM. The levels of significance are *p < 0.05, **p < 0.01, and ***p < 0.001.

model for studying neuronal regeneration and NSC plasticity. By focusing on stem cell populations, we also identified how Aβ42, the hallmark of Alzheimer's disease, affects these cell types and which genes and pathways are altered upon Aβ42 toxicity. Because the zebrafish brain can enhance its stem cell activity and neurogenesis in Alzheimer's disease conditions, understanding in more detail how Aβ42 affects individual cells would certainly enhance our understanding of how a vertebrate brain could counteract Alzheimer's pathology and propose previously unidentified targets for clinical use or drug development.

In mammals, radial glial cells give rise to astrocytes during the second wave of neurogenesis (Hansen et al., 2010; Kriegstein and Alvarez-Buylla, 2009; Urbán and Guillemot, 2014). In fish, however, radial glia remain as such morphologically, and, by definition, there is no astrocyte in the telencephalon (Adolf et al., 2006; Ganz et al., 2012; Grandel et al., 2006; März et al., 2010; Mueller et al., 2004). In our study, the PC populations were almost entirely positive for S100beta, a canonical marker for astrocytes in mammals (Doetsch et al., 1999). Therefore, we believe that marker-based interpretation of a cell type in evolutionary terms cannot be performed and that, in zebrafish, radial glial cells take over astrocytic functions. Additionally, in our tSNE analyses, no progenitor cluster generated a branch that could be considered astrocytes. Therefore, we believe that there are no astrocytes in the telencephalon, which supports previous studies (Barbosa et al., 2015; Grupp et al., 2010; Kaslin et al., 2008; Kizil et al., 2012b; Lam et al., 2009; Mueller and Wullimann, 2009; Rothenaigner et al., 2011; Than-Trong and Bally-Cuif, 2015). In mice, astrocytes also co-segregate with NSCs in single-cell analyses (Artegiani et al., 2017), suggesting that, even in species where astrocytes are evident, without specific sorting for these cells, they cannot be distinguished from existing cell types.

Our analyses subdivided the *her4.1*-positive PC population, which had previously been considered a uniform cell type: radial glia (Kroehne et al., 2011; März et al., 2010; Than-Trong and Bally-Cuif, 2015; Yeo et al., 2007). We identified 9 sub-clusters, 2 of which are ventral neuroepithelial cell types that are not radial glia, which supports previous findings (Kaslin et al., 2008). Another two clusters are neuroblasts, which separate according to their proliferative status. Pre-neuroblasts express almost identical markers as proliferating neuroblasts but also share common markers with the remaining five sub-clusters of progenitors, from which they emanate. Whether PCs are lineage-restricted or multipotent has been an intriguing question (Alvarez-Buylla et al., 2002; Laywell et al., 2000; Raj et al., 2018; Temple, 2001). Studies in salamanders have proposed that regenerative masses of progenitors are strictly lineage-restricted and remember their original identities (Antos and Tanaka, 2010; Kragl et al., 2009), whereas, in mammals, where neurogenic competency and potency of the neural progenitors decline with age, progenitors are lineage-restricted in adult stages and multipotent in embryonic development (Costa et al., 2010; Götz, 2012, 2015). Our study in zebrafish suggests that neuroblasts—cells that are proliferative and leading to actual neurogenesis—cluster into a single population. We therefore propose that the mode of neurogenesis and lineage competency of the zebrafish brain involves transition from a single, rather homogeneous cell population (neuroblasts) with common molecular landmarks and represents the embryonic mode of neurogenesis in mammals. This also suggests that zebrafish can be used as a viable comparative tool for mammalian brains to understand the molecular programs that would mimic the early embryonic stages of neurogenesis in adult stages. Because one of the aims in regenerative therapies is to rejuvenate the adult mammalian brain and to impose regenerative ability back to it (Gage et al., 2016; Katsimpardi et al., 2014; Wyss-Coray, 2016), the adult zebrafish brain would serve as an excellent model, with its endogenous life-long neurogenic competency and regenerative ability.

Our results provide complex and multi-layered information that can be retrieved from our accompanying website (http://www.kizillab.org/singlecell). First, it provides refinement of the cell types and progenitor states in the adult zebrafish telencephalon. This will allow investigation of certain regions or cell types at a higher resolution and can allow cell-specific investigation of biological phenomena. Our analyses of the pathways that are active in certain clusters in homeostatic states of the fish brain also provide candidate signaling pathways that can be investigated in detail. Parallels between our results and previous literature as well as our validation studies confirm the fidelity of our analyses and interpretations. In addition to known signaling molecules, our data provide extensive resources for identification of new molecules and cellular interactions in the adult fish brain. Additionally, our analyses with Aβ42 and IL-4 treatment provide unprecedented information regarding the stem cell plasticity and regenerative output of the fish brain in Alzheimer's conditions.

## STAR★METHODS

Detailed methods are provided in the online version of this paper and include the following:

- KEY RESOURCES TABLE
- CONTACT FOR REAGENT AND RESOURCE SHARING
- EXPERIMENTAL MODEL AND SUBJECT DETAILS
  - Ethics statement
  - Animals
- METHOD DETAILS
  - Cerebroventricular microinjection
  - Cell Dissociation and sorting
  - Droplet encapsulation sequencing
  - Data Analysis by Seurat
  - Monocle analysis of progenitor cells
  - Identification of cell types
  - GO-term analyses
  - Construction of interaction maps
- QUANTIFICATION AND STATISTICAL ANALYSES
- DATA AND SOFTWARE AVAILABILITY
  - R scripts

### SUPPLEMENTAL INFORMATION

Supplemental Information can be found online at https://doi.org/10.1016/j.celrep.2019.03.090.

## ACKNOWLEDGMENTS

This work was supported by German Center for Neurogenerative Disease (DZNE) and the Helmholtz Association Young Investigator Award (VH-NG-1021 to C.K.), Deutsche Forschungsgemeinschaft (DFG) (KI1524/6, KI1524/10, and KI1524/11 to C.K.), CRTD, TU Dresden (FZ-111 and 043_261518 to C.K.). Neurowind e.V. supported the open access publication of this manuscript. C.K. dedicates this paper to Adnan Kizil.

## AUTHOR CONTRIBUTIONS

M.I.C. and C.K. conceived and designed the experiments. P.B. performed cerebroventricular microinjections. Y.Z. provided the amyloid peptide. S.R., A.P., and A.D. performed single-cell sequencing. M.I.C. performed bioinformatics analyses. M.I.C., P.B., and C.K. performed immunohistochemical staining and quantifications. M.I.C. and C.K. generated the supplemental website. C.K. supervised the study, acquired funding, and wrote the manuscript. C.K. and M.I.C. revised the manuscript.

## DECLARATION OF INTERESTS

The authors declare no competing interests.

Received: October 8, 2018
Revised: February 21, 2019
Accepted: March 25, 2019
Published: April 23, 2019

## REFERENCES

Adolf, B., Chapouton, P., Lam, C.S., Topp, S., Tannhäuser, B., Strähle, U., Götz, M., and Bally-Cuif, L. (2006). Conserved and acquired features of adult neurogenesis in the zebrafish telencephalon. Dev. Biol. *295*, 278–293.

Alunni, A., and Bally-Cuif, L. (2016). A comparative view of regenerative neurogenesis in vertebrates. Development *143*, 741–753.

Alunni, A., Krecsmarik, M., Bosco, A., Galant, S., Pan, L., Moens, C.B., and Bally-Cuif, L. (2013). Notch3 signaling gates cell cycle entry and limits neural stem cell amplification in the adult pallium. Development *140*, 3335–3347.

Alvarez-Buylla, A., Seri, B., and Doetsch, F. (2002). Identification of neural stem cells in the adult vertebrate brain. Brain Res. Bull. *57*, 751–758.

Antos, C.L., and Tanaka, E.M. (2010). Vertebrates that regenerate as models for guiding stem cells. Adv. Exp. Med. Biol. *695*, 184–214.

Artegiani, B., Lyubimova, A., Muraro, M., van Es, J.H., van Oudenaarden, A., and Clevers, H. (2017). A Single-Cell RNA Sequencing Study Reveals Cellular and Molecular Dynamics of the Hippocampal Neurogenic Niche. Cell Rep. *21*, 3271–3284.

Barbosa, J.S., Sanchez-Gonzalez, R., Di Giaimo, R., Baumgart, E.V., Theis, F.J., Götz, M., and Ninkovic, J. (2015). Neurodevelopment. Live imaging of adult neural stem cell behavior in the intact and injured zebrafish brain. Science *348*, 789–793.

Bhattarai, P., Thomas, A.K., Cosacak, M.I., Papadimitriou, C., Mashkaryan, V., Froc, C., Reinhardt, S., Kurth, T., Dahl, A., Zhang, Y., and Kizil, C. (2016). IL4/STAT6 signaling activates neural stem cell proliferation and neurogenesis upon Amyloid-β42 aggregation in adult zebrafish brain. Cell Rep. *17*, 941–948.

Bhattarai, P., Thomas, A.K., Cosacak, M.I., Papadimitriou, C., Mashkaryan, V., Zhang, Y., and Kizil, C. (2017a). Modeling Amyloid-β42 Toxicity and Neurodegeneration in Adult Zebrafish Brain. J. Vis. Exp. Published online October 25, 2017. https://doi.org/10.3791/56014.

Bhattarai, P., Thomas, A.K., Zhang, Y., and Kizil, C. (2017b). The effects of aging on Amyloid-β42-induced neurodegeneration and regeneration in adult zebrafish brain. Neurogenesis (Austin) *4*, e1322666.

Butler, A., Hoffman, P., Smibert, P., Papalexi, E., and Satija, R. (2018). Integrating single-cell transcriptomic data across different conditions, technologies, and species. Nat. Biotechnol. *36*, 411–420.

Cacialli, P., Gueguen, M.M., Coumailleau, P., D'Angelo, L., Kah, O., Lucini, C., and Pellegrini, E. (2016). BDNF Expression in Larval and Adult Zebrafish Brain: Distribution and Cell Identification. PLoS ONE *11*, e0158057.

Chellaiah, A., Yuan, W., Chellaiah, M., and Ornitz, D.M. (1999). Mapping ligand binding domains in chimeric fibroblast growth factor receptor molecules. Multiple regions determine ligand binding specificity. J. Biol. Chem. *274*, 34785–34794.

Cosacak, M.I., Papadimitriou, C., and Kizil, C. (2015). Regeneration, Plasticity, and Induced Molecular Programs in Adult Zebrafish Brain. BioMed Res. Int. *2015*, 769763.

Costa, M.R., Götz, M., and Berninger, B. (2010). What determines neurogenic competence in glia? Brain Res. Brain Res. Rev. *63*, 47–59.

Diotel, N., Vaillant, C., Gueguen, M.M., Mironov, S., Anglade, I., Servili, A., Pellegrini, E., and Kah, O. (2010). Cxcr4 and Cxcl12 expression in radial glial cells of the brain of adult zebrafish. J. Comp. Neurol. *518*, 4855–4876.

Diotel, N., Vaillant, C., Gabbero, C., Mironov, S., Fostier, A., Gueguen, M.M., Anglade, I., Kah, O., and Pellegrini, E. (2013). Effects of estradiol in adult neurogenesis and brain repair in zebrafish. Horm. Behav. *63*, 193–207.

Diotel, N., Rodriguez Viales, R., Armant, O., März, M., Ferg, M., Rastegar, S., and Strähle, U. (2015). Comprehensive expression map of transcription regulators in the adult zebrafish telencephalon reveals distinct neurogenic niches. J. Comp. Neurol. *523*, 1202–1221.

Doetsch, F. (2003). The glial identity of neural stem cells. Nat. Neurosci. *6*, 1127–1134.

Doetsch, F., Caillé, I., Lim, D.A., García-Verdugo, J.M., and Alvarez-Buylla, A. (1999). Subventricular zone astrocytes are neural stem cells in the adult mammalian brain. Cell *97*, 703–716.

Falcon, S., and Gentleman, R. (2007). Using GOstats to test gene lists for GO term association. Bioinformatics *23*, 257–258.

Farrell, J.A., Wang, Y., Riesenfeld, S.J., Shekhar, K., Regev, A., and Schier, A.F. (2018). Single-cell reconstruction of developmental trajectories during zebrafish embryogenesis. Science *360*, eaar3131.

Gage, F.H., Guarente, L.P., and Wagers, A.J. (2016). Aging and Rejuvenation: Insights from Rusty Gage, Leonard Guarente, and Amy Wagers. Trends Mol. Med. *22*, 633–634.

Ganz, J., Kaslin, J., Hochmann, S., Freudenreich, D., and Brand, M. (2010). Heterogeneity and Fgf dependence of adult neural progenitors in the zebrafish telencephalon. Glia *58*, 1345–1363.

Ganz, J., Kaslin, J., Freudenreich, D., Machate, A., Geffarth, M., and Brand, M. (2012). Subdivisions of the adult zebrafish subpallium by molecular marker analysis. J. Comp. Neurol. *520*, 633–655.

Goldman, J.E. (2012). Astrocyte development. In Neuroglia, H. Kettenmann and B.R. Ransom, eds. (Oxford University Press), pp. 137–147.

Götz, M. (2012). Radial glial cells. In Neuroglia, H. Kettenmann and B.R. Ransom, eds. (Oxford University Press), pp. 50–61.

Götz, M., Sirko, S., Beckers, J., and Irmler, M. (2015). Reactive astrocytes as neural stem or progenitor cells: In vivo lineage, In vitro potential, and Genome-wide expression analysis. Glia *63*, 1452–1468.

Grandel, H., Kaslin, J., Ganz, J., Wenzel, I., and Brand, M. (2006). Neural stem cells and neurogenesis in the adult zebrafish brain: origin, proliferation dynamics, migration and cell fate. Dev. Biol. *295*, 263–277.

Grupp, L., Wolburg, H., and Mack, A.F. (2010). Astroglial structures in the zebrafish brain. J. Comp. Neurol. *518*, 4277–4287.

Hansen, D.V., Lui, J.H., Parker, P.R., and Kriegstein, A.R. (2010). Neurogenic radial glia in the outer subventricular zone of human neocortex. Nature *464*, 554–561.

Jiao, S., Dai, W., Lu, L., Liu, Y., Zhou, J., Li, Y., Korzh, V., and Duan, C. (2011). The conserved clusterin gene is expressed in the developing choroid plexus under the regulation of notch but not IGF signaling in zebrafish. Endocrinology *152*, 1860–1871.

Johansson, C.B., Momma, S., Clarke, D.L., Risling, M., Lendahl, U., and Frisén, J. (1999). Identification of a neural stem cell in the adult mammalian central nervous system. Cell *96*, 25–34.

Kaslin, J., Ganz, J., and Brand, M. (2008). Proliferation, neurogenesis and regeneration in the non-mammalian vertebrate brain. Philos. Trans. R. Soc. Lond. B Biol. Sci. *363*, 101–122.

Kaslin, J., Ganz, J., Geffarth, M., Grandel, H., Hans, S., and Brand, M. (2009). Stem cells in the adult zebrafish cerebellum: initiation and maintenance of a novel stem cell niche. J. Neurosci. *29*, 6142–6153.

Katsimpardi, L., Litterman, N.K., Schein, P.A., Miller, C.M., Loffredo, F.S., Wojtkiewicz, G.R., Chen, J.W., Lee, R.T., Wagers, A.J., and Rubin, L.L. (2014). Vascular and neurogenic rejuvenation of the aging mouse brain by young systemic factors. Science *344*, 630–634.

Kizil, C. (2018). Mechanisms of Pathology-Induced Neural Stem Cell Plasticity and Neural Regeneration in Adult Zebrafish Brain. Curr. Pathobiol. Rep. *6*, 71–77.

Kizil, C., and Brand, M. (2011). Cerebroventricular microinjection (CVMI) into adult zebrafish brain is an efficient misexpression method for forebrain ventricular cells. PLoS ONE *6*, e27395.

Kizil, C., Dudczig, S., Kyritsis, N., Machate, A., Blaesche, J., Kroehne, V., and Brand, M. (2012a). The chemokine receptor cxcr5 regulates the regenerative neurogenesis response in the adult zebrafish brain. Neural Dev. *7*, 27.

Kizil, C., Kaslin, J., Kroehne, V., and Brand, M. (2012b). Adult neurogenesis and brain regeneration in zebrafish. Dev. Neurobiol. *72*, 429–461.

Kizil, C., Kyritsis, N., Dudczig, S., Kroehne, V., Freudenreich, D., Kaslin, J., and Brand, M. (2012c). Regenerative neurogenesis from neural progenitor cells requires injury-induced expression of Gata3. Dev. Cell *23*, 1230–1237.

Kizil, C., Iltzsche, A., Kaslin, J., and Brand, M. (2013). Micromanipulation of gene expression in the adult zebrafish brain using cerebroventricular microinjection of morpholino oligonucleotides. J. Vis. Exp. *75*, e50415.

Klämbt, C. (2012). Evolution of glial cells. In Neuroglia, H. Kettenmann and B.R. Ransom, eds. (Oxford University Press), pp. 5–11.

Kragl, M., Knapp, D., Nacu, E., Khattak, S., Maden, M., Epperlein, H.H., and Tanaka, E.M. (2009). Cells keep a memory of their tissue origin during axolotl limb regeneration. Nature *460*, 60–65.

Kriegstein, A., and Alvarez-Buylla, A. (2009). The glial nature of embryonic and adult neural stem cells. Annu. Rev. Neurosci. *32*, 149–184.

Kroehne, V., Freudenreich, D., Hans, S., Kaslin, J., and Brand, M. (2011). Regeneration of the adult zebrafish brain from neurogenic radial glia-type progenitors. Development *138*, 4831–4841.

Kyritsis, N., Kizil, C., Zocher, S., Kroehne, V., Kaslin, J., Freudenreich, D., Iltzsche, A., and Brand, M. (2012). Acute inflammation initiates the regenerative response in the adult zebrafish brain. Science *338*, 1353–1356.

Lam, C.S., März, M., and Strähle, U. (2009). gfap and nestin reporter lines reveal characteristics of neural progenitors in the adult zebrafish brain. Dev. Dyn. *238*, 475–486.

Laywell, E.D., Rakic, P., Kukekov, V.G., Holland, E.C., and Steindler, D.A. (2000). Identification of a multipotent astrocytic stem cell in the immature and adult mouse brain. Proc. Natl. Acad. Sci. USA *97*, 13883–13888.

Lindsey, B.W., Darabie, A., and Tropepe, V. (2012). The cellular composition of neurogenic periventricular zones in the adult zebrafish forebrain. J. Comp. Neurol. *520*, 2275–2316.

März, M., Chapouton, P., Diotel, N., Vaillant, C., Hesl, B., Takamiya, M., Lam, C.S., Kah, O., Bally-Cuif, L., and Strähle, U. (2010). Heterogeneity in progenitor cell subtypes in the ventricular zone of the zebrafish adult telencephalon. Glia *58*, 870–888.

März, M., Schmidt, R., Rastegar, S., and Strähle, U. (2011). Regenerative response following stab injury in the adult zebrafish telencephalon. Dev. Dyn. *240*, 2221–2231.

Mueller, T., and Wullimann, M.F. (2009). An evolutionary interpretation of teleostean forebrain anatomy. Brain Behav. Evol. *74*, 30–42.

Mueller, T., Vernier, P., and Wullimann, M.F. (2004). The adult central nervous cholinergic system of a neurogenetic model animal, the zebrafish Danio rerio. Brain Res. *1011*, 156–169.

Ogino, T., Sawada, M., Takase, H., Nakai, C., Herranz-Pérez, V., Cebrián-Silla, A., Kaneko, N., García-Verdugo, J.M., and Sawamoto, K. (2016). Characterization of multiciliated ependymal cells that emerge in the neurogenic niche of the aged zebrafish brain. J. Comp. Neurol. *524*, 2982–2992.

Olstad, E.W., Ringers, C., Hansen, J.N., Wens, A., Brandt, C., Wachten, D., Yaksi, E., and Jurisch-Yaksi, N. (2019). Ciliary beating compartmentalizes cerebrospinal fluid flow in the brain and regulates ventricular development. Curr. Biol. *29*, 229–241.e6.

Pacary, E., Martynoga, B., and Guillemot, F. (2012). Crucial first steps: the transcriptional control of neuron delamination. Neuron *74*, 209–211.

Pandey, S., Shekhar, K., Regev, A., and Schier, A.F. (2018). Comprehensive identification and spatial mapping of habenular neuronal types using single-cell RNA-seq. Curr. Biol. *28*, 1052–1065.e7.

Papadimitriou, C., Celikkaya, H., Cosacak, M.I., Mashkaryan, V., Bray, L., Bhattarai, P., Brandt, K., Hollak, H., Chen, X., He, S., et al. (2018). 3D Culture Method for Alzheimer's Disease Modeling Reveals Interleukin-4 Rescues Abeta42-Induced Loss of Human Neural Stem Cell Plasticity. Dev. Cell *46*, 85–101.e8.

Pollen, A.A., Nowakowski, T.J., Chen, J., Retallack, H., Sandoval-Espinosa, C., Nicholas, C.R., Shuga, J., Liu, S.J., Oldham, M.C., Diaz, A., et al. (2015). Molecular identity of human outer radial glia during cortical development. Cell *163*, 55–67.

Qiu, X., Hill, A., Packer, J., Lin, D., Ma, Y.A., and Trapnell, C. (2017). Single-cell mRNA quantification and differential analysis with Census. Nat. Methods *14*, 309–315.

Raj, B., Wagner, D.E., McKenna, A., Pandey, S., Klein, A.M., Shendure, J., Gagnon, J.A., and Schier, A.F. (2018). Simultaneous single-cell profiling of lineages and cell types in the vertebrate brain. Nat. Biotechnol. *36*, 442–450.

Ramilowski, J.A., Goldberg, T., Harshbarger, J., Kloppmann, E., Lizio, M., Satagopam, V.P., Itoh, M., Kawaji, H., Carninci, P., Rost, B., and Forrest, A.R. (2015). A draft network of ligand-receptor-mediated multicellular signalling in human. Nat. Commun. *6*, 7866.

Reinhardt, L., Kordes, S., Reinhardt, P., Glatza, M., Baumann, M., Drexler, H.C.A., Menninger, S., Zischinsky, G., Eickhoff, J., Frob, C., et al. (2019). Dual Inhibition of GSK3beta and CDK5 Protects the Cytoskeleton of Neurons from Neuroinflammatory-Mediated Degeneration In Vitro and In Vivo. Stem Cell Reports *12*, 502–517.

Rothenaigner, I., Krecsmarik, M., Hayes, J.A., Bahn, B., Lepier, A., Fortin, G., Götz, M., Jagasia, R., and Bally-Cuif, L. (2011). Clonal analysis by distinct viral vectors identifies bona fide neural stem cells in the adult zebrafish telencephalon and characterizes their division properties and fate. Development *138*, 1459–1469.

Satija, R., Farrell, J.A., Gennert, D., Schier, A.F., and Regev, A. (2015). Spatial reconstruction of single-cell gene expression data. Nat. Biotechnol. *33*, 495–502.

Shimizu, Y., Ueda, Y., and Ohshima, T. (2018). Wnt signaling regulates proliferation and differentiation of radial glia in regenerative processes after stab injury in the optic tectum of adult zebrafish. Glia *66*, 1382–1394.

Skelly, D.A., Squiers, G.T., McLellan, M.A., Bolisetty, M.T., Robson, P., Rosenthal, N.A., and Pinto, A.R. (2018). Single-Cell Transcriptional Profiling Reveals Cellular Diversity and Intercommunication in the Mouse Heart. Cell Rep. *22*, 600–610.

Sleptsova-Friedrich, I., Li, Y., Emelyanov, A., Ekker, M., Korzh, V., and Ge, R. (2001). fgfr3 and regionalization of anterior neural tube in zebrafish. Mech. Dev. *102*, 213–217.

Spassky, N., Merkle, F.T., Flames, N., Tramontin, A.D., García-Verdugo, J.M., and Alvarez-Buylla, A. (2005). Adult ependymal cells are postmitotic and are derived from radial glial cells during embryogenesis. J. Neurosci. *25*, 10–18.

Sternberg, J.R., Prendergast, A.E., Brosse, L., Cantaut-Belarif, Y., Thouvenin, O., Orts-Del'Immagine, A., Castillo, L., Djenoune, L., Kurisu, S., McDearmid,

J.R., et al. (2018). Pkd2l1 is required for mechanoception in cerebrospinal fluid-contacting neurons and maintenance of spine curvature. Nat. Commun. *9*, 3804.

Temple, S. (2001). The development of neural stem cells. Nature *414*, 112–117.

Than-Trong, E., and Bally-Cuif, L. (2015). Radial glia and neural progenitors in the adult zebrafish central nervous system. Glia *63*, 1406–1428.

Tincer, G., Mashkaryan, V., Bhattarai, P., and Kizil, C. (2016). Neural stem/progenitor cells in Alzheimer's disease. Yale J. Biol. Med. *89*, 23–35.

Topp, S., Stigloher, C., Komisarczuk, A.Z., Adolf, B., Becker, T.S., and Bally-Cuif, L. (2008). Fgf signaling in the zebrafish adult brain: association of Fgf activity with ventricular zones but not cell proliferation. J. Comp. Neurol. *510*, 422–439.

Urbán, N., and Guillemot, F. (2014). Neurogenesis in the embryonic and adult brain: same regulators, different roles. Front. Cell. Neurosci. *8*, 396.

Wyss-Coray, T. (2016). Ageing, neurodegeneration and brain rejuvenation. Nature *539*, 180–186.

Yeo, S.Y., Kim, M., Kim, H.S., Huh, T.L., and Chitnis, A.B. (2007). Fluorescent protein expression driven by her4 regulatory elements reveals the spatiotemporal pattern of Notch signaling in the nervous system of zebrafish embryos. Dev. Biol. *301*, 555–567.

Zheng, G.X., Lau, B.T., Schnall-Levin, M., Jarosz, M., Bell, J.M., Hindson, C.M., Kyriazopoulou-Panagiotopoulou, S., Masquelier, D.A., Merrill, L., Terry, J.M., et al. (2016). Haplotyping germline and cancer genomes with high-throughput linked-read sequencing. Nat. Biotechnol. *34*, 303–311.

Zupanc, G.K. (2008). Adult neurogenesis and neuronal regeneration in the brain of teleost fish. J. Physiol. Paris *102*, 357–373.

# STAR★METHODS

## KEY RESOURCES TABLE

| REAGENT or RESOURCE | SOURCE | IDENTIFIER |
|---|---|---|
| Antibodies | | |
| Anti-GFP | Abcam | Cat# ab13970, RRID:AB_300798 |
| Anti-PCNA | Dako | Cat# M0879, RRID:AB_2160651 |
| Anti-S100β | Dako | Cat# Z0311, RRID:AB_10013383 |
| Goat anti-Chicken IgY (H+L) Secondary Antibody, Alexa Fluor 488 | Thermo Fischer | Cat# A11039, RRID:AB_142924 |
| Goat anti-Rabbit IgG (H+L) Cross-Adsorbed Secondary Antibody, Alexa Fluor 488 | Thermo Fischer | Cat# A11008; RRID: AB_143165 |
| Goat anti-Mouse IgG (H+L) Cross-Adsorbed Secondary Antibody, Alexa Fluor 488 | Thermo Fischer | Cat# A-11001, RRID:AB_2534069 |
| Goat anti-Mouse IgG (H+L) Cross-Adsorbed Secondary Antibody, Alexa Fluor 555 | Thermo Fischer | Cat# A21422; RRID: AB_141822 |
| Chemicals, Peptides, and Recombinant Proteins | | |
| Transportan signal peptide-coupled Amyloid-β42 | (Bhattarai et al., 2016) | N/A |
| Recombinant human Protein IL4 | Thermo Fischer | Cat# PHC0044 |
| Recombinant human Protein FGF8 | Thermo Fischer | Cat# PHG0184 |
| Bovine Serum Albumin (BSA) | Sigma | Cat# A2153 |
| MESAB | Sigma | Cat# A5040 |
| Critical Commercial Assays | | |
| Neural Tissue Dissociation Kit (P) | Miltenyi | Cat# 130-092-628 |
| 10X Chromium Kit | 10X Genomics | Cat# 1000092 |
| Deposited Data | | |
| Single cell transcriptome | This paper | GEO: GSE118577 |
| Experimental Models: Organisms/Strains | | |
| Tg(her4.1:GFP) transgenic zebrafish line | (Yeo et al., 2007) | N/A |
| Software and Algorithms | | |
| Cell Ranger 2.01 | (Zheng et al., 2016) | RRID:SCR_016957 |
| GOstats_2.48.0 | (Falcon and Gentleman, 2007) | http://gostat.wehi.edu.au; RRID: SCR_008535 |
| monocle_2.10.1 | (Qiu et al., 2017) | N/A |
| Seurat_2.3.4 | (Butler et al., 2018) | RRID:SCR_016341 |
| R scripts for data analyses | This paper | https://www.kizillab.org/resources |
| R version 3.5.2 (2018-12-20) | N/A | RRID:SCR_001905 |
| x86_64-w64-mingw32/x64 (64-bit) | N/A | https://sourceforge.net/, RRID:SCR_004365 |
| Transcriptomics dataset website | This paper | https://www.kizillab.org/singlecell |

## CONTACT FOR REAGENT AND RESOURCE SHARING

Further information and requests for resources and reagents should be directed to and will be fulfilled by the Lead Contact, Caghan Kizil (caghan.kizil@dzne.de).

## EXPERIMENTAL MODEL AND SUBJECT DETAILS

### Ethics statement

All animal experiments were performed under the permission of Landesdirektion Dresden with the following permit numbers: TVV-52/2015 with all relevant amendments.

### Animals

Transgenic zebrafish expressing GFP under the *her4*.1 promoter (Tg(her4.1:GFP, Yeo et al., 2007) was used for sorting progenitors and the rest of the telencephalon. 6 months post fertilization (mpf) female fish were used for analyses.

## METHOD DETAILS

### Cerebroventricular microinjection

Tg(her4.1:GFP) zebrafish were injected through a slit generated over the optic tectum using a barbed end 30-gauge needle (Bhattarai et al., 2016; Kizil and Brand, 2011; Kizil et al., 2013). Glass capillary filled with injection liquid was inserted into the cerebrospinal space of the adult brain and 1 μl of the solution was injected. Fish were injected with either with PBS (control), Aβ42 (20 μM) or Interleukin-4 (1 μM), and were kept at 14 hr light/10 hr dark cycle in normal water system for 24 hours. FGF8 was injected at 0.2 mg/ml final concentration. Experimental fish were sacrificed using 0.2% MESAB according to the animal experimentation permits.

### Cell Dissociation and sorting

The telencephalon of the fish were dissected in ice-cold PBS and directly dissociated with Neural Tissue Dissociation Kit (Miltenyi) at 28.5°C as described previously (Bhattarai et al., 2016). After dissociation, cells were filtered through 40 μM cell strainer into 10 mL 2% BSA in PBS, centrifuged at 300 g for 10 min and cells resuspended in 4% BSA in PBS. Viability indicator (Propidium iodide) and GFP were used to sort viable GFP(+) or GFP(-) cells by FACS. The resulting single cell suspension was promptly loaded on the 10X Chromium system (Zheng et al., 2016). 10X libraries were prepared as per the manufacturer's instructions. The raw sequencing data was processed by the cell ranger software provided by the 10X genomics with the default options. The reads were aligned to zebrafish reference transcriptome (ENSEMBL Zv10, release 91) and eGFP CDS (with arbitrary ensemble ID; ENSDARG99999999999). The resulting matrices were used as input for downstream data analysis by Seurat (Butler et al., 2018).

### Droplet encapsulation sequencing

To prepare the cells for droplet-based sequencing, 2700 GFP-positive and 2700 GFP-negative cells were flow-sorted into a coated tubes containing 2 μl saline solution with 0.04 % Bovine serum albumin (BSA). Subsequently, the single cell suspension was carefully mixed with reverse transcription mix before loading the cells on the 10X Genomics Chromium system. During the encapsulation, the cells were lysed within the droplet and they released polyadenylated RNA bound to the barcoded bead, which was encapsulated with the cell. Following the guidelines of the 10x Genomics user manual, the droplets were directly subjected to reverse transcription, the emulsion was broken and cDNA was purified using Silane beads. After the amplification of cDNA with 10 cycles, purification and quantification was performed.

The 10X Genomics single cell RNA-sequencing library preparation - involving fragmentation, dA-tailing, adapter ligation, and 12-cycle indexing PCR – was performed. After quantification, the libraries were sequenced on an Illumina NextSeq 550 machine using a HighOutput flowcell in paired-end mode (R1: 26 cycles; I1: 8 cycles; R2: 57 cycles), thus generating 80-125 million fragments. The raw sequencing data was then processed with the 'count' command of the Cell Ranger software provided by 10X Genomics. The option of '–expect-cells' was set to 2700 (all other options were used as per default). To build the reference for Cell Ranger, zebrafish genome (GRCz10) as well as gene annotation (Ensembl 91) were downloaded from Ensembl and the annotation was filtered with the 'mkgtf' command of Cell Ranger (options: '–attribute=gene_biotype:protein_coding –attribute=gene_biotype:lincRNA –attribute=gene_biotype:antisense'). Genome sequence and filtered annotation were then used as input to the 'mkref' command of Cell Ranger to build the appropriate CellRanger Reference.

### Data Analysis by Seurat

All matrices were read by Read10X function; cell names were re-named as sample names and the column number, to trace back cells if required. First, we removed all ribosomal RNA genes, then we filtered out cells as following; cell with more than 15000 UMI or less than 1000 UMI, cells with less than 500 or more than 2500 unique genes, cells with more than 6% mitochondrial genes. The genes found in less than 5 cells were filtered out. Moreover, we removed cells with potential of mulitplet. The remaining cells and genes were used for downstream analysis for all samples. The data normalized by using ''LogNormalize'' method, data scaled with ''scale.factor = 1e4.'' For each datasets variable genes found with FindVariableGenes with the following options mean.function = ExpMean, dispersion.function = LogVMR, x.low.cutoff = 0.125, x.high.cutoff = 10, y.cutoff = 0.5. The top1000 most highly variable genes from each sample were merged, mitochondrial genes were removed. Then, the intersection of these genes with all genes in each samples were used for CCA analysis. The 3 Seurat objects and the variable genes found above were used to generate a new Seurat object with RunMultiCCA function, using num.ccs = 30. The canonical correlation strength were calculated using num.dims = 1:30 and the samples were aligned using dims.align = 1:10. The cell clusters were found using aligned CCA and 1:10 dims, with higher resolution 1.0. The cell clusters were shown on 2D using t-SNE (RunTSNE function). By using some general markers, we found 4 major cell types; Progenitor Cells (PCs) [*fabp7a*+], Immune cells (Im) [*lcp1*+, *pfn1*+], Oligodenrocytes / Progenitor Cells (OPC/OD_1, OPC/OD_2), and Neuron (*sv2a*+, *synpr*+). The marker genes for these 5 cell poplations were calculated by using FindAllMarkers function with options min.pct = 0.25, thresh.use = 0.25. The Progenitor cells or Neurons were separated from all other

cells and PCs or Neuronal cell clusters were identified using aforementioned steps with some changes; instead of num.dims = 10, num.dims = 20 were used. The marker genes for PCs or Neuronal cell types were identified as above.

### Monocle analysis of progenitor cells

In order to identify cell trajectories on pseudotime, we converte the Progentor cells Seurat object to Monocle (Qiu et al., 2017). The estimated size factor set to 1.0 as the data were already normalized by Seurat. We used the genes used for CCA analysis for ordering in monocle, with max_components = 4. The cells were colored as the colors on Seurat TSNE plots.

### Identification of cell types

Feature plots were generated by Seurat software and cell types were determined by the expression of marker genes that define specific cell types.

### GO-term analyses

We used the all marker genes with False Detection Rate < 0.1 for Gene Ontology analysis and KEGG pathway analysis using GOStats (1.7.4) (Falcon and Gentleman, 2007) and GSEABase (1.40.1), p value < 0.05 as threshold as described previously (Papadimitriou et al., 2018). To determine the differentially expressed genes (DEGs) after Aβ42 and IL4 treatment, we used FindMarkers function using cell cluster that have at least 3 cells from all samples. Then, we used the p value < 0.05 for significantly expressed genes. These genes were used for GO and pathway analysis using the scripts that are available on www.kizillab.org/resources.

### Construction of interaction maps

For the ligand-receptor interaction, we downloaded all Ligand and receptors from a previous publication (Ramilowski et al., 2015) (http://fantom.gsc.riken.jp/5/suppl/Ramilowski_et_al_2015/vis/#/hive), and orthologs for zebrafish were found using BiomaRt of ENSEMBL. The ligand-receptor for zebrafish were used for downstream analysis as following; for cell-cell interaction, all ligands found in 20% of a cell types were chosen, then their receptors were identified in all cell types. If a ligand-receptor pathway was found, then we draw a direction from the cell with the ligand to the cells with the receptor. We used igraph in R to draw interaction map as previously described (Skelly et al., 2018). In order to show the lost and/or new interaction after treatment, we calculated all the interaction for PBS and the treatment (Aβ42 or IL4) and then generated an interaction maps from all interaction of PBS and the treatment. Then, we colored the edges as cyan (lost after treatment), purple (induced after treatment) and black that are not affected by the treatment; but may be differentially expressed.

## QUANTIFICATION AND STATISTICAL ANALYSES

Images from histological sections were acquired using Zeiss ZEN software in Zeiss Apotome, Leica SP5 confocal microscope or using AxioScanner slide scanner. Counting was performed on acquired images in a double-blinded manner. The statistical analyses were performed using GraphPad Prism and two-tailed Student's t tests. The levels of significance were *p < 0.05, **p < 0.01, and ***p < 0.001. In all graphs, means ± standard errors of the means were shown. The data conforms to normal distribution as determined by Pearson's chi-square test.

## DATA AND SOFTWARE AVAILABILITY

All feature plots, VLN plots, GO terms and pathway analyses, and interaction maps and the list of genes associated with these analyses can be found on the accompanying website (http://www.kizillab.org/singlecell), which can be accessed freely.

All raw data are deposited to GEO (http://www.ncbi.nlm.nih.gov/geo/) with accession number GEO: GSE118577.

### R scripts

All scripts used for the data analysis can be found on https://www.kizillab.org/resources.